Analysis of (p,p'x) reactions by semi-classical distorted-wave (SCDW) model with single particle wave functions for Woods-Saxon potential

Sun Weili [a)*], Y. Watanabe[a)], K. Ogata[c)], M. Kohno[b)], and M. Kawai[c)]

[a)]*Department of Energy Conversion Engineering, Kyushu University, Kasuga, Fukuoka 816-8580, Japan*

[b)]*Physics Division, Kyushu Dental College, Kitakyushu 803-8580, Japan*

[c)]*Department of Physics, Kyushu University, Fukuoka 812-8581, Japan*

[*]*email: sun@aees.kyushu-u.ac.jp*

Multi-step direct (p,p'x) processes are analyzed in terms of SCDW model that is extended so as to use single particle wave functions for finite range potentials, i.e., harmonic oscillator and Woods-Saxson potentials, by means of the Wigner transform of one-body mixed density. The effects of momentum distributions of target nucleons on the multi-step direct processes are discussed. The calculated angular distributions including multi-step processes up to 3-step are compared with experimental data of ^{90}Zr(p,p'x) reactions at incident energies of 80 and 160 MeV.

I. Introduction

In recent years, proton nuclear data in the intermediate energy region are required for various engineering and medical applications. In this energy region, the multistep direct (MSD) processes in preequilibrium nuclear reactions become important. We applied SCDW model to analyze the experimental data of MSD processes in (p,p'x) reactions [1-4]. The results showed underestimation of the angular distributions at forward and backward angles. It was found that one of the reasons was the use of a local density Fermi-gas (LFG) model to describe the nuclear states. Hence, SCDW model was reformulated in terms of the Wigner transform of one-body mixed density, so that more realistic single-particle wave functions of target nucleons can be used. The first calculations with the single-particle wave functions for harmonic oscillator (HO) potential [5] showed that the cross sections at forward and backward angles were enhanced as expected, because of the higher momentum components of target nucleons. However, they were somewhat small compared with the experimental data.

In the present work, we use the single-particle wave functions for Woods-Saxon (WS) potential and carry out the calculations for ^{90}Zr(p,p'x) reactions at two incident energies of 80 and 160 MeV. The analysis is extended to include the MSD processes up to 3-step. We discuss the effects of the momentum distributions of target nucleons on MSD angular distributions for three cases, LFG, HO, and WS.

II. SCDW model with Wigner transform of one-body mixed density

The detailed description and formulation of SCDW model have been given in elsewhere[1-4]. Here, we explain the extension of SCDW model with the Wigner transform of one-body mixed denisty.

In each step of MSD, a target nucleon collides with a leading particle and is excited from

a single particle state $\phi_\alpha(\mathbf{r})$ at energy ε_α below the Fermi level, F, to a state $\phi_\beta(\mathbf{r})$ at ε_β above F. Then, the 1-step cross section is written by

$$\frac{\partial^2\sigma^{(1)}}{\partial E_f \partial\Omega_f} = \frac{4\mu^2}{(2\pi\hbar^2)^2}\frac{k_f}{k_i}\int d\mathbf{r}d\mathbf{r}'d\mathbf{r}_0 d\mathbf{r}_0' \chi_f^{(-)*}(\mathbf{r}_0)v(\mathbf{r}_0,\mathbf{r})\chi_i^{(+)}(\mathbf{r}_0) \times\chi_f^{(-)}(\mathbf{r}_0')v(\mathbf{r}_0',\mathbf{r}')\chi_i^{(+)*}(\mathbf{r}_0')K(\mathbf{r},\mathbf{r}') \ , \quad (1)$$

where the non-local kernel $K(\mathbf{r},\mathbf{r}')$ is given by

$$K(\mathbf{r},\mathbf{r}') = \sum_{\beta>F}\sum_{\alpha<F}\phi_\beta^*(\mathbf{r})\phi_\alpha(\mathbf{r})\phi_\beta(\mathbf{r}')\phi_\alpha^*(\mathbf{r}')\delta(\varepsilon_\beta-\varepsilon_\alpha-\omega) \ , \quad (2)$$

where ω is the energy transfer and the definition of other quantities is same as used in Refs. [3,4]. Due to the closure property of the ϕ, $K(\mathbf{r},\mathbf{r}')$ is appreciable only when $\mathbf{r}\approx\mathbf{r}'$. If the LFG model is used to describe the nuclear states, the ϕ are approximated by plane waves within a small cell centered at $\mathbf{r}\approx\mathbf{r}'$. In terms of the Wigner transform of one body density matrix [6], we can treat more realistic single particle wave functions in the finite range potentials, such as HO or WS potential, in SCDW model. In Ref. [5], we gave the expressions of Wigner transform for numerical calculations with a variation method. Here, we describe how to incorporate them into SCDW model on the basis of Ref. [7].

Let us start from general single particle model. The wave functions of struck nucleon, $\phi_\alpha(\mathbf{r})$ and $\phi_\beta(\mathbf{r})$, satisfy the following Schrödinger equation:

$$h_\gamma\phi_\gamma = (T_\gamma+U_\gamma)\phi_\gamma = \varepsilon_\gamma\phi_\gamma \qquad \text{for} \quad \gamma=\alpha \text{ or } \beta \ . \quad (3)$$

Then, $K(\mathbf{r},\mathbf{r}')$ can be re-written by

$$K(\mathbf{r},\mathbf{r}') = \delta(h_\beta(\mathbf{r})-h_\alpha(\mathbf{r})-\omega)\sum_{\alpha<F}\phi_\alpha(\mathbf{r})\phi_\alpha^*(\mathbf{r}')\sum_{\beta>F}\phi_\beta^*(\mathbf{r})\phi_\beta(\mathbf{r}') \ , \quad (4)$$

where $h_\alpha(\mathbf{r})$ operates on $\phi_\alpha(\mathbf{r})$, $h_\beta(\mathbf{r})$ on $\phi_\beta^*(\mathbf{r})$.

The Wigner transforms corresponding to hole and particle states, respectively, are given as follows:

$$f_h(\mathbf{k}_\alpha,\mathbf{r}) = \int e^{-i\mathbf{k}_\alpha\mathbf{s}}\sum_{\alpha<F}\phi_\alpha(\mathbf{r}+\mathbf{s}/2)\phi_\alpha^*(\mathbf{r}-\mathbf{s}/2)d\mathbf{s} \ , \quad (5)$$

$$f_p(\mathbf{k}_\beta,\mathbf{r}) = \int e^{-i\mathbf{k}_\beta\mathbf{s}}\sum_{\beta>F}\phi_\beta(\mathbf{r}+\mathbf{s}/2)\phi_\beta^*(\mathbf{r}-\mathbf{s}/2)d\mathbf{s} \ , \quad (6)$$

where $\mathbf{k}_\alpha$ is the momentum of struck nucleon before collision and $\mathbf{k}_\beta$ the one after collision. By making inverse Fourier transform, $\sum_{\alpha<F}\phi_\alpha(\mathbf{r})\phi_\alpha^*(\mathbf{r}')$ and $\sum_{\beta>F}\phi_\beta^*(\mathbf{r})\phi_\beta(\mathbf{r}')$ are obtained by

$$\sum_{\alpha<F}\phi_\alpha(\mathbf{r})\phi_\alpha^*(\mathbf{r}') = \frac{1}{(2\pi)^3}\int e^{i\mathbf{k}_\alpha(\mathbf{r}-\mathbf{r}')}f_h(\mathbf{k}_\alpha,(\mathbf{r}+\mathbf{r}')/2)d\mathbf{k}_\alpha \ , \quad (7)$$

$$\sum_{\beta>F}\phi_\beta^*(\mathbf{r})\phi_\beta(\mathbf{r}') = \frac{1}{(2\pi)^3}\int e^{-i\mathbf{k}_\beta(\mathbf{r}-\mathbf{r}')} f_p(\mathbf{k}_\beta,(\mathbf{r}+\mathbf{r}')/2)d\mathbf{k}_\beta . \quad (8)$$

If we assume the potential U_α acting on struck nucleon before collision is approximately equal to U_β acting on struck nucleon after collision, then

$$h_\beta(\mathbf{r}) - h_\alpha(\mathbf{r}) \approx T_\beta(\mathbf{r}) - T_\alpha(\mathbf{r}) \ . \quad (9)$$

Furthermore, if $f\ (\mathbf{k},\mathbf{r})$ is a slowly varying function of **r**, we can make an approximation

$$T_\alpha(\mathbf{r})e^{i\mathbf{k}_\alpha(\mathbf{r}-\mathbf{r}')} f_h(\mathbf{k}_\alpha,(\mathbf{r}+\mathbf{r}')/2) \approx (\hbar^2k_\alpha^2/2\mu)e^{i\mathbf{k}_\alpha(\mathbf{r}-\mathbf{r}')} f_h(\mathbf{k}_\alpha,(\mathbf{r}+\mathbf{r}')/2) \quad (10)$$

$$T_\beta(\mathbf{r})e^{-i\mathbf{k}_\beta(\mathbf{r}-\mathbf{r}')} f_p(\mathbf{k}_\beta,(\mathbf{r}+\mathbf{r}')/2) \approx (\hbar^2k_\beta^2/2\mu)e^{-i\mathbf{k}_\beta(\mathbf{r}-\mathbf{r}')} f_p(\mathbf{k}_\beta,(\mathbf{r}+\mathbf{r}')/2) \quad (11)$$

Under these approximations, $K^{(c)}(\mathbf{r},\mathbf{r}')$ is finally given by

$$K^{(c)}(\mathbf{r},\mathbf{r}') \approx \frac{1}{(2\pi)^6}\int d\mathbf{k}_\alpha d\mathbf{k}_\beta e^{i\mathbf{q}(\mathbf{r}-\mathbf{r}')} f_h^{(c)}(\mathbf{k}_\alpha,\mathbf{R})[1-f_h^{(c)}(\mathbf{k}_\beta,\mathbf{R})]\delta(\hbar^2k_\beta^2/2\mu - \hbar^2k_\alpha^2/2\mu - \omega), \quad (12)$$

where c denotes neutron or proton shell, $\mathbf{q}=\mathbf{k}_\alpha-\mathbf{k}_\beta$, and $\mathbf{R}=(\mathbf{r}+\mathbf{r}')/2$. In deriving Eq.(12), the normalization condition for all states is used, which leads to $f_p(\mathbf{k}_\beta,\mathbf{R}) = 1-f_h(\mathbf{k}_\beta,\mathbf{R})$. For convenience, we write $f^{(c)}(\mathbf{k},\mathbf{R}) = f_h^{(c)}(\mathbf{k},\mathbf{R})$ hereafter.

As did in Refs. [1-4], we use a local semi-classical approximation to distorted wave $\chi_c^{(\pm)}(\mathbf{r}_0')$ in Eq. (1) we also make the approximation $f^{(c)}(\mathbf{k},\mathbf{R}) \approx f^{(c)}(\mathbf{k},\mathbf{r})$. Thus, the final 1-step cross section is given as follows:

$$\frac{\partial^2\sigma^{(1)}}{\partial E_f\partial\Omega_f} = \left(\frac{A}{A+1}\right)^2\int d\mathbf{r}\left|\chi_i^{(+)}(\mathbf{r})\right|^2\left|\chi_f^{(-)}(\mathbf{r})\right|^2\frac{k_f/k_f(\mathbf{r})}{k_i/k_i(\mathbf{r})}\left[\frac{\partial^2\sigma}{\partial E_f\partial\Omega_f}\right]_{\mathbf{r}}\rho^{(c)}(\mathbf{r}), \quad (13)$$

where the product of local average N-N scattering cross section and density is given by

$$\left[\frac{\partial^2\sigma}{\partial E_f\partial\Omega_f}\right]_{\mathbf{r}}\rho^{(c)}(\mathbf{r}) = \frac{8}{(2\pi)^3}\frac{k_f(\mathbf{r})}{k_i(\mathbf{r})}\int d\mathbf{k}_\alpha\int d\mathbf{k}_\beta\left[\frac{\partial\sigma}{\partial\Omega}\right]_{NN} f^{(c)}(\mathbf{k}_\alpha,\mathbf{r})[1-f^{(c)}(\mathbf{k}_\beta,\mathbf{r})]$$
$$\times\delta(\mathbf{k}_f(\mathbf{r})+\mathbf{k}_\beta-\mathbf{k}_i(\mathbf{r})-\mathbf{k}_\alpha)\delta(\hbar^2k_\beta^2/2\mu-\hbar^2k_\alpha^2/2\mu-\omega), \quad (14)$$

where $\left[\frac{\partial\sigma}{\partial\Omega}\right]_{NN}$ is the two-body N-N scattering cross section.

The extension to the 2- and 3-step processes is straightforward with Eq. (14) for each collision point.

III. Results and Discussion

Figs.1 and 2 show the momentum distributions, $n(k)$, of target nucleons for HO and WS potentials compared with that given by the LFG model in linear and logarithmic scales, respectively. It should be noted that the one for WS potential is different from the previous calculation[5], because the number of Gaussian basis as the variational function is different between both the calculations, i.e., 20 in the present calculation and 10 in the previous one. Enough large number of Gaussian basis is necessary for precise calculations of the Wigner transform when the momentum k is larger than 2 fm^{-1}. The other parameters used in the calculation are the same as those in Ref. [5]. One can see that the momentum distribution by the LFG model contains too much low momentum components and no higher momentum components above the Fermi momentum. On the other hand, the momentum distributions calculated by both finite range potentials show remarkable reduction of low momentum components below 0.3 fm^{-1} and existence of higher momentum components compared with LFG. Also, one can see some differences between momentum distributions for HO and WS potentials in the high momentum region.

The SCDW model with the Wigner transform was applied to the ^{90}Zr(p,p'x) reaction at two incident energies of 80 and 160 MeV in order to investigate the effects of the nucleon momentum distribution on MSD processes. The basic input parameters, i.e., distorting potentials, N-N scattering cross sections and nuclear density, were the same as in the previous calculations [3,4]. Fig.3 shows comparisons of individual multi-step cross sections calculated for three cases, LFG, HO, and WS, for the incident energy of 160 MeV. The 1-step cross sections calculated with HO and WS potentials are enhanced remarkably at backward angles compared with the LFG result that drops steeply at backward angles. The 1-step cross sections for HO and WS are also larger than those for LFG at very forward angles near 0 degree. In addition, some differences are seen between both HO and WS results; 1-step cross section for WS is larger than that for HO at backward angles, but the 2-and 3-step cross sections show the opposite behavior at backward angles.

For three cases, (a) LFG, (b) HO and (c) WS, the SCDW calculations including 3-step process are compared with experimental data in Fig. 4. The results with HO and WS potentials are in better agreement with the experimental data[8] than that with LFG at backward angles. Also, both results lead to some reduction of cross sections around 30 degree corresponding to the quasi-elastic scattering angle and improve the shape of angular distributions in the entire angular region. It is worthwhile to note that the sum of individual cross sections for HO is almost same as that for WS, even if the individual cross sections are different, particularly for the 1-step process, as shown in Fig. 3. For both cases of HO and WS, the cross sections summed up to 3-step are somewhat smaller than the experimental data. This might suggest the contribution from higher MSD steps.

Fig. 5 shows comparisons of SCDW calculations for three cases with experimental data[9] at the incident energy of 80 MeV. Similar behavior in individual cross sections can be seen as in Figs.3 and 4. The summed cross sections for both HO and WS show much better agreement with the experimental data at backward angles than those for LFG.

IV. Summary

The SCDW model with the Wigner transform of one-body mixed density was applied to the analysis of the ^{90}Zr(p,p'x) reaction at 80 and 160 MeV. In the analysis, HO and WS potentials was employed as the finite range potential to use more realistic single-partile wave functions than the LFG model in SCDW. The SCDW calculations with HO and WS potentials

obviously improve the underestimation to the experimental data at backward angles, which is seen in the calculation with LFG. The 1-step cross sections calculated with WS potential increase at very forward and backward angles, more than those of HO potential. However, the sum of individual cross sections is almost same for both potentials, because 2- and 3-step cross sections calculated with W-S potential are smaller than those with HO potential at backward angles. This result shows that the momentum distribution of target nucleons affects strongly the 1-step cross sections at the forward and backward angles and the effect becomes weak as the step number increases. Our calculation still somewhat underestimates the experimental data at backward angles even if the higher momentum components of target nucleons are considered, which should be further investigated. In addition, it will be necessary to investigate the validation of the approximations used in Eqs. (10) and (11) in Sec. II.

Acknowledgment

This work is partly supported by Grand-in-Aid Scientific Research of the Ministry of Education, Science and Culture (No. 09558059).

References

[1] Y.L. Luo and M. Kawai, Phys. Rev.C **43**, 2367 (1991).
[2] M. Kawai and H.A. Weidenmüller, Phys. Rev.C **45**, 1856 (1992).
[3] Y. Watanabe and M. Kawai, Nucl. Phys. **A560**, 43 (1993).
[4] Y. Watanabe et al., to be submitted to Phys. Rev. C, (1998).
[5] Sun Weili et al., JEARI-Conf. 98-003, p.282 (1998).
[6] See, for example, H. Feshbach, *Theoretical Nuclear Physics, Nuclear Reactions* (John Wiley and sons, 1992).
[7] M. Kawai et al., *Proceedings of the Fifteenth International Workshop on Nuclear Theory*, Rila mountains, Sofia, Bulgaria, 10-16 June,1996.
[8] W.A. Richter et al., Phys. Rev. C **49**, 1001 (1994).
[9] A.A. Cowley et al., Phys. Rev. C **43**, 678 (1991).

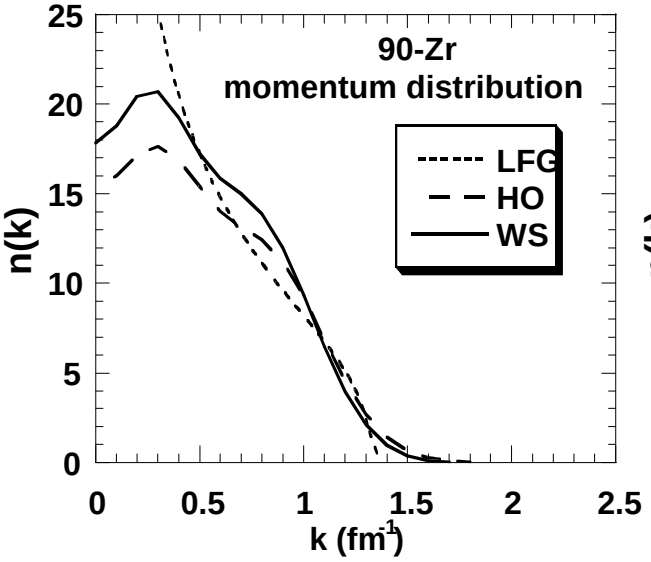

Fig.1 Momentum Distribution of target nucleon for ^{90}Zr in a linear scale

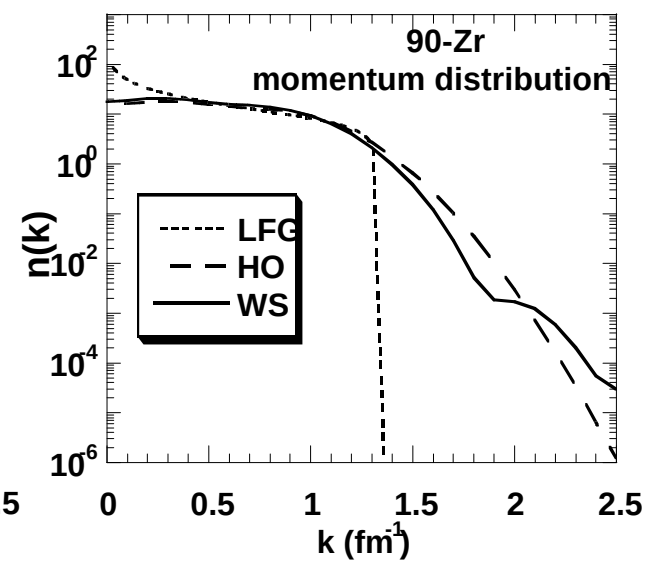

Fig.2 Same as Fig.1 but in a logarithmic scale

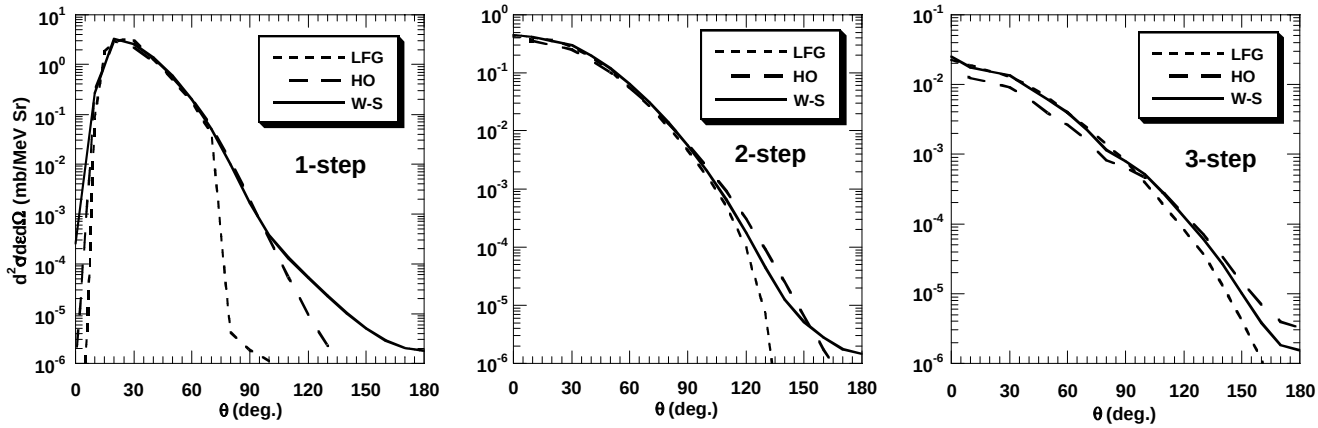

Fig.3 Comparison of individual multistep cross sections for three cases, (a) LFG model, (b) HO and (c)WS for the ^{90}Zr(p,p'x) reaction at an incident energy of 160 MeV and an outgoing energy of 120 MeV.

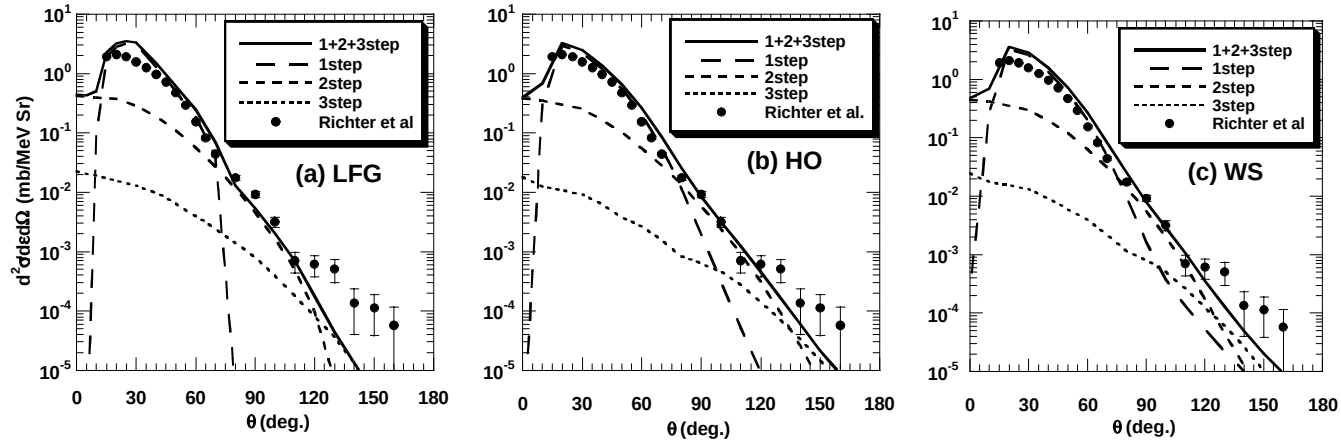

Fig.4 Comparison of calculation with experimental data for three cases, (a) LFG model, (b) HO and (c) WS for the ^{90}Zr(p,p'x) reaction at an incident energy of 160 MeV and an outgoing energy of 120 MeV. The experimental data are taken from Ref.[8].

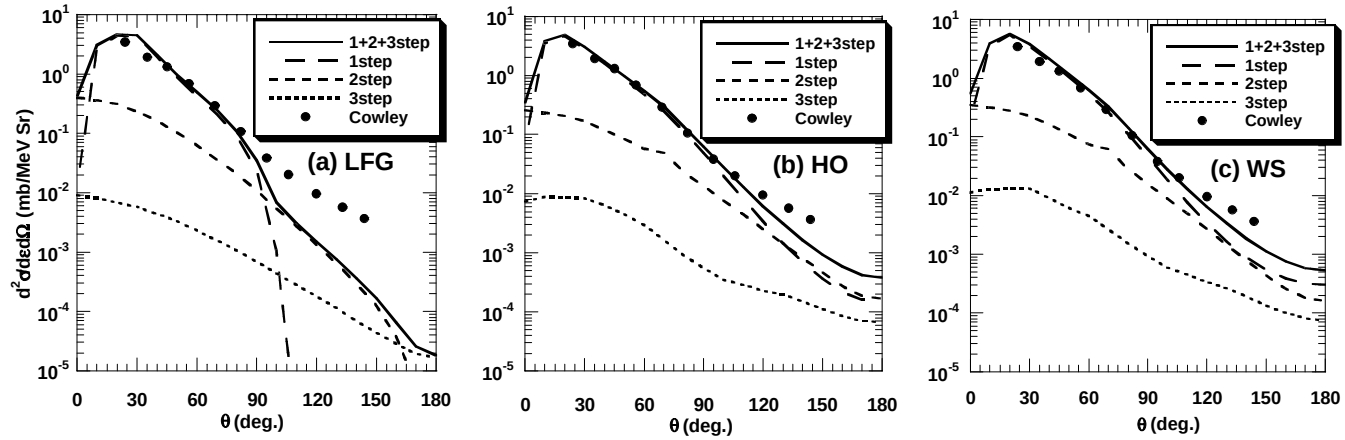

Fig.5 Same as Fig. 4, but at an incident energy of 80 MeV and an outgoing energy of 60 MeV. The experimental data are taken from Ref.[9].